arXiv:1402.6086v3 [cond-mat.quant-gas] 10 Dec 2014

Persistent currents in a two-component Bose-Einstein condensate confined in a ring potential

J. Smyrnakis[1], M. Magiropoulos[1], Nikolaos K. Efremidis[2], and G. M. Kavoulakis[1]
[1] *Technological Education Institute of Crete, P.O. Box 1939, GR-71004, Heraklion, Greece*
[2] *Department of Applied Mathematics, University of Crete, GR-71004, Heraklion, Greece*
(Dated: December 11, 2014)

We present variational and numerical solutions for the problem of stability of persistent currents in a two-component Bose-Einstein condensate of distinguishable atoms which rotate in a ring potential. We consider the general class of solutions of constant density in the two components separately, thus providing an alternative approach of the solution of the same problem given recently by Zhigang Wu and Eugene Zaremba [Phys. Rev. A **88**, 063640 (2013)]. Our approach provides a physically transparent solution of this delicate problem. Finally, we give a unified and simple picture of the lowest-energy state of the system for large values of the coupling.

PACS numbers: 05.30.Jp, 03.75.Lm, 67.60.Bc

I. INTRODUCTION

The problem of persistent currents in a toroidal/annular potential of Bose-Einstein condensed atoms (of a single species) has attracted a lot of attention in recent years. The experiments of Refs. [1–7] have managed to create persistent currents in such trapping geometries and thus realize probably the most simple superfluid system that has been realized in the laboratory. These experiments are thus ideal for studying the fascinating effect of frictionless flow, which is one of the many problems associated with the more general effect of "superfluidity".

A non-trivial extension of the problem of the stability of persistent currents is the one of mixtures of two distinguishable species. Remarkably, this problem has been realized and examined in the recent experiment of Ref. [8], which makes its theoretical study even more interesting. In Ref. [9] it was shown that the stability of persistent currents is strongly affected by the addition of a second component. If A and B are the labels of the two species and $\tilde{\ell} = \ell\hbar = (L/N)\hbar$ is the angular momentum per particle, with $L\hbar = (L_A + L_B)\hbar$ being the total angular momentum and $N = N_A + N_B$ being the total population of the two species, it was shown that in the range $0 \leq \ell \leq 1$ stability of persistent currents is possible for $\ell = \max(x_A, x_B)$, with $x_i = N_i/N$. In what follows below we assume that $x_A > x_B$.

According to Ref. [9], the energy spectrum consists of a periodic part, plus an envelope parabolic function of ℓ, in analogy with the problem of a single component, as shown by Felix Bloch [10]. It is thus natural to examine the stability of persistent currents at the corresponding values of ℓ which are higher than unity, i.e., at $\ell = m + x_A$, with $m = 1, 2, \ldots$ It turns out that for these values of ℓ the persistent currents are very fragile, even for very small concentrations of the minority component [9].

Motivated by Ref. [9], two recent papers by Anoshkin, Wu, and Zaremba [11] and by Wu and Zaremba [12] examined the same problem theoretically. In Ref. [12] it was shown that while for $\ell = m + x_A$, with $m = 1, 2, \ldots$ persistent currents are absent, indeed, still they are possible for $\ell = m x_A$. In the language of the present study they investigated the stability of persistent currents around the combination $(\Psi_A, \Psi_B) = (\Phi_m, \Phi_0)$, where $\Phi_m = e^{im\theta}/\sqrt{2\pi R}$, with θ being the azimuthal angle and $m = 0, \pm 1, \pm 2, \ldots$ To do this, the authors of Ref. [12] found solutions of the coupled nonlinear equations satisfied by the two order parameters and evaluated their energy. Interestingly, the problem considered here may also be viewed from the point of view of solitary-wave solutions, where bound states of "gray" and "bright" solitary waves in the two components propagate together along the torus/annulus [13].

In the theoretical analysis of Refs. [9] and [12] the parameters γ_{AA}, γ_{BB}, and γ_{AB} which characterize the coupling between the species AA, BB, and AB respectively, were assumed to be equal to each other. Here $\gamma_{ij} = 4N a_{ij} R/S$, where a_{ij} $(i = A, B)$ is the scattering length for elastic atom-atom collisions (assumed to be positive), S is the cross section of the toroidal/annular potential, which is approximated as a zero-width, ring potential of radius R. In our analysis which follows below we assume equal values for the couplings γ_{ij} and equal masses, $M_A = M_B = M$. Under these assumptions the condition for phase coexistence (which is crucial in our analysis) is satisfied [9]. We stress that the problem of persistent currents in the case of unequal couplings and/or unequal masses has a very different behavior, as we will show in a future publication.

In this study we examine the problem of stability of persistent currents, starting with the states $(\Psi_A, \Psi_B) = (\Phi_m, \Phi_n)$. Clearly this pair of states has an angular momentum $\ell = m x_A + n x_B$. The benefit from the present study is that it provides an alternative solution of the one given in Ref. [12], as it avoids solving the two coupled nonlinear differential equations satisfied by Ψ_A and Ψ_B. As a result, this procedure is also physically transparent. As we explain in more detail below, the combination $(\Psi_A, \Psi_B) = (\Phi_m, \Phi_n)$ is not necessarily the lowest-energy (yrast) state for the specific value of $\ell = m x_A + n x_B$, and thus one has to investigate this problem, too.

In what follows we first investigate in Sec. II the question of persistent currents for $\ell \to (mx_A + nx_B)^-$, assuming that the pair of states $(\Psi_A, \Psi_B) = (\Phi_m, \Phi_n)$ constitute the yrast state for the specific value of ℓ. It turns out that only the case $n = 0$ may give stability of the currents [12]. Then, in Sec. III we investigate the conditions which make the pair $(\Psi_A, \Psi_B) = (\Phi_m, \Phi_0)$ the actual yrast state. We thus derive two phase boundaries in the plane diagram which involves the variables x_A and γ. In Sec. IV we present our numerical results. In Sec. V we examine the lowest-energy state of the system in the limit of large values of the coupling, showing that the total density is homogeneous for all values of the angular momentum. Finally, in Sec. VI we give a summary and a discussion of our results.

II. STABILITY OF PERSISTENT CURRENTS FOR $\ell \to (mx_A + nx_B)^-$

The Hamiltonian of the system that we consider is

$$H = -\sum_{i=1}^{N_A} \frac{\hbar^2}{2MR^2}\frac{\partial^2}{\partial\theta_{A,i}^2} - \sum_{j=1}^{N_B} \frac{\hbar^2}{2MR^2}\frac{\partial^2}{\partial\theta_{B,j}^2} + \frac{1}{2}U_{AA}\sum_{i\neq j=1}^{N_A}\delta(\theta_{A,i}-\theta_{A,j}) + \frac{1}{2}U_{BB}\sum_{i\neq j=1}^{N_B}\delta(\theta_{B,i}-\theta_{B,j}) + U_{AB}\sum_{i=1}^{N_A}\sum_{j=1}^{N_B}\delta(\theta_{A,i}-\theta_{B,j}). \quad (1)$$

Here $U_{ij} = 4\pi\hbar^2 a_{ij}/(MRS)$ (with $i, j = A, B$), are the matrix elements for zero-energy elastic atom-atom collisions.

To determine the yrast state around the value of the angular momentum $\ell = \ell_0 \equiv mx_A + nx_B$, we first assume that $(\Psi_A, \Psi_B) = (\Phi_m, \Phi_n)$, $m > n \geq 0$, is the yrast state for $\ell = \ell_0$; the validity of this assumption is actually investigated in Sec. III. For values of $\ell \approx \ell_0$, the order parameters Ψ_A and Ψ_B will have admixtures of additional states, however while the amplitudes of Φ_m, Φ_n will be of order unity, the amplitudes of these other states will be small, much smaller than unity. Furthermore, since we are looking for the yrast state, the combination of the (additional) states which will enter Ψ_A will be of the form $c_{m-q}\Phi_{m-q} + c_m\Phi_m + c_{m+q}\Phi_{m+q}$ and correspondingly for Ψ_B, with $q = 1, 2, \ldots$ The reason for this "symmetric" choice is that there is a process where two atoms with angular momentum m scatter to two other states with angular momentum $m + q$ and $m - q$ (angular momentum is conserved in the collisions). The corresponding term in the interaction energy will be proportional to $c_{m-q}c_m^2c_{m+q}$, which may become negative, and thus lower the energy. Finally, q is equal to unity, since the states Φ_{m-1} and Φ_{m+1} have the lowest kinetic energy, while the matrix element of the interaction that is associated with the above scattering process is independent of the angular momentum. Therefore, we consider the order parameters [9]

$$\Psi_A = c_{m-1}\Phi_{m-1} + c_m\Phi_m + c_{m+1}\Phi_{m+1}, \quad (2)$$
$$\Psi_B = d_{n-1}\Phi_{n-1} + d_n\Phi_n + d_{n+1}\Phi_{n+1}, \quad (3)$$

where the six coefficients satisfy the obvious conditions of particle normalization and of fixed angular momentum ℓ. As stated also above, $c_{m\pm1}$ and $d_{n\pm1}$ are assumed to be small, and thus linearisation is possible. We thus evaluate the expectation value of the Hamiltonian in the states Ψ_A and Ψ_B and then perform this linearisation to find a quadratic expression for the energy per particle, which is

$$\frac{E}{N\epsilon} - \frac{\gamma}{2} = x_A[m^2 + (1-2m)c_{m-1}^2 + (1+2m)c_{m+1}^2] + x_B[n^2 + (1-2n)d_{n-1}^2 + (1+2n)d_{n+1}^2] + \gamma[x_A^2(c_{m-1}+c_{m+1})^2 + x_B^2(d_{n-1}+d_{n+1})^2 + 2x_Ax_B(c_{m-1}+c_{m+1})(d_{n-1}+d_{n+1})]. \quad (4)$$

Here $\epsilon = \hbar^2/(2MR^2)$ is the kinetic energy and $\gamma = 4NaR/S$, which was defined also above, is the ratio between the interaction energy of the cloud with a homogeneous density $N/(2\pi R)$ of $N = N_A + N_B$ atoms and the kinetic energy ϵ.

The angular momentum ℓ in the states of Eqs. (2) and (3) is given by $\ell = \ell_0 + x_A(c_{m+1}^2 - c_{m-1}^2) + x_B(d_{n+1}^2 - d_{n-1}^2)$. Defining $g = x_A(c_{m+1}^2 - c_{m-1}^2) + x_B(d_{n+1}^2 - d_{n-1}^2)$, then $\ell - \ell_0 = g$. Let us thus introduce the Lagrange multiplier λ and extremize $E/(N\epsilon) + \lambda g$. The resulting equations are

$$\begin{aligned}
-(2m-1)c_{m-1} + \gamma[x_A(c_{m-1}+c_{m+1}) + x_B(d_{n-1}+d_{n+1})] - \lambda c_{m-1} &= 0\\
(2m+1)c_{m+1} + \gamma[x_A(c_{m-1}+c_{m+1}) + x_B(d_{n-1}+d_{n+1})] + \lambda c_{m+1} &= 0\\
-(2n-1)d_{n-1} + \gamma[x_A(c_{m-1}+c_{m+1}) + x_B(d_{n-1}+d_{n+1})] - \lambda d_{n-1} &= 0\\
(2n+1)d_{n+1} + \gamma[x_A(c_{m-1}+c_{m+1}) + x_B(d_{n-1}+d_{n+1})] + \lambda d_{n+1} &= 0.
\end{aligned} \quad (5)$$

Demanding that the determinant of the above homogeneous linear system of equations to vanish (so that there are non-zero solutions) we get that $\gamma = f(\lambda)$, where

$$f(\lambda) \equiv \frac{1}{2}\frac{[(\lambda+2m)^2-1][(\lambda+2n)^2-1]}{x_A[(\lambda+2n)^2-1] + x_B[(\lambda+2m)^2-1]}. \quad (6)$$

In examining the above condition $\gamma = f(\lambda)$ one has to distinguish between the cases $m = n+1$ and $m > n+1$. Starting with the case $m = n+1$, it turns out that

$$\gamma = f(\lambda) = \frac{1}{2}\frac{(\lambda+2n+3)[(\lambda+2n)^2-1]}{\lambda - 1 + 2n + 4x_B}. \quad (7)$$

The function $f(\lambda)$ has one asymptote, while Eq. (7) has three roots for sufficiently large values of γ. Figure 1(a) shows an example, where we have chosen $m = 1$, $n = 0$, $x_A = 0.99$, and $x_B = 0.01$ in this case, while the horizontal dashed line corresponds to $\gamma = 15$. However, not all three roots are acceptable. In order for the angular momentum ℓ to be smaller than ℓ_0 [since we are interested in the case $\ell \to \ell_0^-$], only the two larger roots are acceptable. This may be seen by examining the sign of

$$\ell - \ell_0 = x_A(c_{m+1}^2 - c_{m-1}^2) + x_B(d_{n+1}^2 - d_{n-1}^2), \quad (8)$$

where, e.g., c_{m+1}, and $d_{n\pm1}$ may be expressed in terms of c_{m-1} from Eqs. (5).

Furthermore, the slope of the energy per particle (or the "dispersion relation") as function of ℓ is equal to $-\lambda$. This may be seen from the fact that we have extremized $E' = E/(N\epsilon) + \lambda g$ (where $g = \ell - \ell_0$) with respect to ℓ, which implies that $\partial E'/\partial \ell = 0$, or $\partial[E/(N\epsilon)]/\partial \ell = -\lambda$. As a result, the root that gives the stability is the smaller of the two, since we have to choose the one that has the lowest possible energy. Actually, this the one close to the asymptote [see the bullet in Fig. 1(a)], as it was found initially in Ref. [9]. This root tends to $\lambda = -2n + 1 - 4x_B$ for sufficiently large γ. The slope of the dispersion relation is thus $2n - 1 + 4x_B$ and clearly only the case $n = 0$ may give a local energy minimum [9, 11, 12].

Turning to the case $m > n + 1$, there are two asymptotes and four roots [as in Figs. 1(b) and 1(c), where we have chosen $m = 2$ and $n = 0$ in the one case and $m = 3$ and $n = 1$ in the other, with $x_A = 0.99$ and $x_B = 0.01$ in both of them]. The dashed horizontal line again corresponds to the value of $\gamma = 15$. Again, using the same procedure as above, it turns out that among the four possible roots only the higher two are acceptable in this case. Again, the root that determines the stability is the one with the smaller value, and actually it is the larger of the two roots which result from the two asymptotes, indicated as bullets in the plots. For $x_B \to 0$, $\lambda \to -2n+1$, or in other words the slope is $2n-1$. Obviously only the case $n = 0$ may give a local energy minimum, again.

From Fig. 1 it is seen clearly that the root which determines the slope in all three cases is positive for sufficiently large values of the coupling [14] (and thus the slope is negative) only in the top and in the middle, but *not* in the bottom one. This observation is consistent with the fact that only in the case $n = 0$ does one get stability of the currents.

To get the critical value of γ for stability of the persistent currents we thus set $\lambda = 0$ and $n = 0$ in Eq. (6), getting

$$\gamma_{\rm cr} = \frac{1}{2}\frac{4m^2 - 1}{1 - 4m^2 x_B}. \quad (9)$$

The above expression has been derived in Ref. [12], and it has an asymptote at

$$x_{A,\rm cr} = 1 - \frac{1}{4m^2}, \quad (10)$$

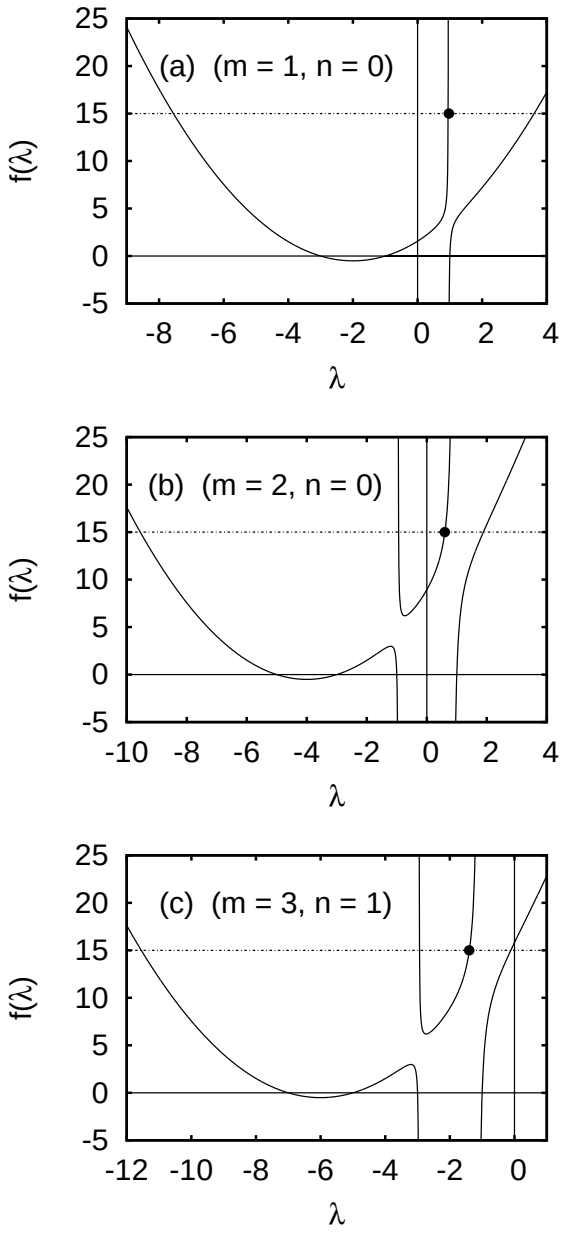

FIG. 1: The function $f(\lambda)$, for (a) $(\Psi_A, \Psi_B) = (\Phi_1, \Phi_0)$, (b) $(\Psi_A, \Psi_B) = (\Phi_2, \Phi_0)$, and (c) $(\Psi_A, \Psi_B) = (\Phi_3, \Phi_1)$. Here $x_A = 0.99$ and $x_B = 0.01$. The horizontal dashed line refers to $\gamma = 15$, while the bullets show the roots which determine the slope in each case.

and therefore x_A is bounded from below by this value. From Eq. (9) it also follows that for $x_A \to 1$,

$$\gamma_{\rm cr} \to 2m^2 - \frac{1}{2}, \quad (11)$$

which is the well-known result for the case of one component (see, e.g., Ref. [9]).

III. YRAST STATE FOR $\ell = mx_A$

In the previous section we assumed implicitly that the pair of states $(\Psi_A, \Psi_B) = (\Phi_m, \Phi_0)$ gives the yrast state for the specific value of the angular momentum $\ell = mx_A$ (n is set equal to zero from now on, since this is the only possible value that may give stability of the currents). For $\ell = m, m + x_B, m + x_A$, and $m + 1$, where $m = 0, \pm 1, \pm 2, \ldots$, the yrast state consists of the pairs $(\Psi_A, \Psi_B) = (\Phi_m, \Phi_m)$, $(\Psi_A, \Psi_B) = (\Phi_m, \Phi_{m+1})$, $(\Psi_A, \Psi_B) = (\Phi_{m+1}, \Phi_m)$, and $(\Psi_A, \Psi_B) = (\Phi_{m+1}, \Phi_{m+1})$, respectively, for any value of γ.

For any other value of the angular momentum the yrast state may consist of a combination of more than one modes for Ψ_A and Ψ_B. For example, for weak interatomic interactions and $0 \leq \ell \leq 1$, the whole yrast state consists only of the two lowest-energy modes, i.e.,

$$\Psi_A = c_0\Phi_0 + c_1\Phi_1, \;\; \Psi_B = d_0\Phi_0 + d_1\Phi_1. \tag{12}$$

On the other hand, for sufficiently strong values of γ, states of a homogeneous density distribution are candidates for being the yrast states, since they minimize the interaction energy. The combination $(\Psi_A, \Psi_B) = (\Phi_m, \Phi_0)$ has a homogeneous density distribution (in each component separately), and this pair of states is indeed the yrast state under the conditions examined below.

To attack this problem one may use the approach described in the previous section, however in the present case the Lagrange multiplier is not set equal to zero, but rather in addition to Eq. (6) (with $n = 0$) self-consistency of Eqs. (5) and the equation for the angular momentum introduces the additional condition

$$4\gamma^2 x_A x_B(\lambda + 2m) + [(\lambda + 2m)^2 - 2\gamma x_A - 1]^2\lambda = 0, \tag{13}$$

where $-2m < \lambda < 0$. Using Eqs. (6) and (13) one may eliminate λ and thus get the critical value of γ, $\gamma_{\rm cr}^{\rm yr}$, as a function of x_A (or equivalently x_B). While this has to be done numerically in general, the limiting cases may be handled analytically. For $x_A \to 1$, then $\lambda \to -1$, and thus

$$\gamma_{\rm cr}^{\rm yr} \to 2m(m-1), \tag{14}$$

in agreement with the result of Wu and Zaremba [12]. Comparing the above value of $\gamma_{\rm cr}^{\rm yr}$ of Eq. (14) with $\gamma_{\rm cr}$, given by Eq. (11), it turns out that $\gamma_{\rm cr}^{\rm yr} < \gamma_{\rm cr}$.

In addition, for large values of γ, then $\lambda \to -2mx_B$ and thus there is one asymptote for the following value of x_A

$$x_{A,{\rm cr}}^{\rm yr} = \frac{1}{2} + \frac{\sqrt{m^2-1}}{2m}, \tag{15}$$

where the solution with the negative sign is not acceptable. Again, the above expression agrees with the one given by Ref. [12]. Comparing this value of $x_{A,{\rm cr}}^{\rm yr}$ from Eq. (15) with $x_{A,{\rm cr}}$ given by Eq. (10) we see that $x_{A,{\rm cr}}^{\rm yr} < x_{A,{\rm cr}}$.

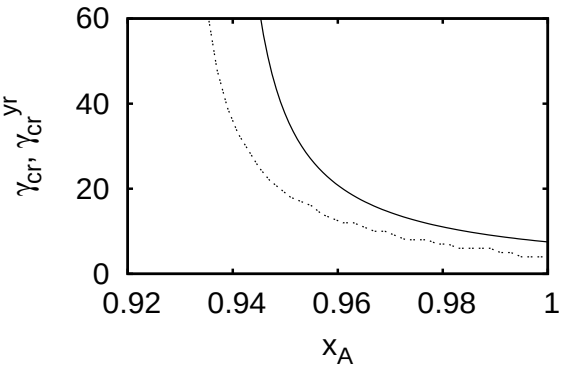

FIG. 2: The two phase boundaries showing $\gamma_{\rm cr}^{\rm yr}$ (dashed curve) and $\gamma_{\rm cr}$ (solid curve) versus x_A, for $(\Psi_A, \Psi_B) = (\Phi_2, \Phi_0)$.

IV. RELATIVE POSITION OF THE TWO PHASE BOUNDARIES

In addition to the above analytical results, we investigated numerically (variationally) the phase boundary for the combination $(\Psi_A, \Psi_B) = (\Phi_m, \Phi_0)$ to become the yrast state (i.e., the question investigated in Sec. III). We have thus kept the two neighbouring states around Φ_m and Φ_0, namely $\Phi_{m\pm1}$ and $\Phi_{\pm1}$.

The result of this calculation is shown as the dashed curve in Fig. 2 for $(m, n) = (2, 0)$. This curve terminates due to numerical reasons. Our results, however, are consistent with the divergence of $\gamma_{\rm cr}^{\rm yr}$ for $x_A \to (2+\sqrt{3})/4 \approx 0.933$, according to Eq. (15). Also, for $x_A \to 1$, $\gamma_{\rm cr}^{\rm yr} \to 4$, in agreement with Eq. (14).

More generally, the whole phase boundary that defines the pair $(\Psi_A, \Psi_B) = (\Phi_m, \Phi_0)$ to be the actual yrast state coincides with the one that results from the analysis presented in Sec. III, i.e., from the solution of Eqs. (6) and (13). In the same figure we have also included the phase boundary for the stability of persistent currents for $(m, n) = (2, 0)$, Eq. (9), [again for $(m, n) = (2, 0)$], where $\gamma_{\rm cr} = 7.5/(16x_A - 15)$.

Thus, the results of this section confirm the general picture which implies that the phase for stability of the currents is always included within the phase for the pair $(\Psi_A, \Psi_B) = (\Phi_m, \Phi_0)$ to be the yrast state, and thus the results of Sec. II – which rely on this crucial assumption – are always valid.

V. A UNIFIED DESCRIPTION OF THE YRAST STATE FOR LARGE VALUES OF THE COUPLING

One remarkable result of the analysis presented in Sec. II is that the slope of the solution that determines the stability of the currents saturates, as it has an upper bound, even for large values of γ. This is easily seen, since the solution that determines the stability comes from ei-

ther the only asymptote in the case $(m = 1, n = 0)$, or one of the two asymptotes for $(m > 1, n = 0)$ of $f(\lambda)$. More specifically, for $x_B \to 0$, the slope of the dispersion relation for large values of γ tends to $-1 + 4x_B$ when $m = 1$, and it tends to $-1 + 2m(m-1)x_B$ when $m > 1$.

To get some insight into this result, let us examine the density, which is given by (since $|c_{m\pm1}| \ll |c_m|$ and $|d_{\pm1}| \ll |d_0|$),

$$\begin{aligned} n_A(\theta) &= \frac{x_A}{2\pi R}[1 + 2(c_{m-1} + c_{m+1})\cos\theta], \\ n_B(\theta) &= \frac{x_B}{2\pi R}[1 + 2(d_{-1} + d_1)\cos\theta]. \end{aligned} \tag{16}$$

Examining the term $x_A(c_{m-1} + c_{m+1}) + x_B(d_{-1} + d_1)$ that appears in the total density $n_A + n_B$, it turns out that this is proportional to

$$\frac{x_A}{(\lambda + 2m)^2 - 1} + \frac{x_B}{\lambda^2 - 1} \propto \gamma^{-1} \to 0, \tag{17}$$

as Eq. (6) implies. In other words, the density variation of $n_A + n_B$ is constant (to order $1/\gamma$), which is the reason for the saturation of the slope: the system manages to maintain its density homogeneous (thus gaining potential energy) at the expense of kinetic energy (due to the extra components $\Phi_{m\pm1}$ and $\Phi_{\pm1}$ in the order parameters Ψ_A and Ψ_B, respectively). For example, for $m = 1$ it may be seen after some algebra that for $\ell \to x_A^-$

$$\frac{E}{N\epsilon} - \frac{\gamma}{2} = \ell + 2(1 - 2x_B)(x_A - \ell). \tag{18}$$

From this formula it follows that the difference $E/N\epsilon - \gamma/2$ is indeed due to the kinetic energy. The same equation also implies that the slope is $-1 + 4x_B$, as we argued also above.

Actually, the homogeneity of the total density is a more general result, which characterizes the yrast state for all values of the angular momentum when the coupling is sufficiently large. As shown in Ref. [9], for $0 \le \ell \le x_B$ and $x_A \le \ell \le 1$, the total density is homogeneous exactly for any value of γ. The same result holds for large values of γ, also for $x_B \le \ell \le x_A$, and thus for *all* values of ℓ.

To demonstrate this, we performed a constrained minimization of the energy of the system considering the trial order parameters $\Psi_A = \sum_{m=-1}^{m=3} c_m \Phi_m$ and $\Psi_B = \sum_{m=-2}^{m=2} d_m \Phi_m$. The imposed constraints were that of particle normalization, of a fixed angular momentum, and finally a constant total density distribution. Figure 3 shows the result of this calculation. In this calculation the coupling drops out completely from the energy, apart from the "background" energy of the homogeneous density distribution [which has an energy $E/(N\epsilon) = \gamma/2$]. This calculation thus demonstrates the saturation that we described earlier. The homogeneity of the total density distribution is expected to become asymptotically exact for large values of γ. In a sense, this effect is analogous to the fermionization of hard-core bosons in one dimension, where the system pays kinetic energy via the fermionization of the bosons, however it gains (more) energy because of the assumed large value of the coupling between the particles.

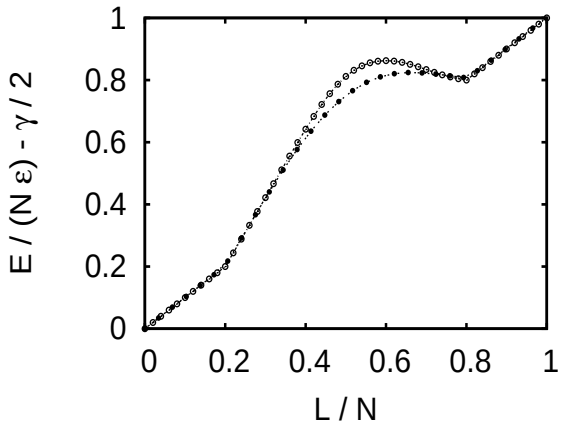

FIG. 3: The dispersion relation for $x_A = 0.8$ and $x_B = 0.2$, with $\gamma = 1250/\pi^2$ in the lower curve and "large" γ in the higher, evaluated through the two methods described in Sec. V.

In the same figure we also show the result of the minimization of the energy via the method of imaginary-time propagation, for some fixed and relatively large value of the coupling $\gamma = 1250/\pi^2$. In this calculation, in order to fix the expectation value of the angular momentum, we have used a Lyapunov functional [15]. While close to each other, the two curves do not coincide, for three reasons. The first one is that they do not correspond to the same value of γ. The second reason is that the one for finite γ is exact up to numerical error. The third reason is that the one for finite γ does not have the constraint of an exactly homogeneous density distribution. As we saw earlier, variations in the total density of order $1/\gamma$ are expected to be present, as we have also confirmed in the numerical solution we have found with the method of the imaginary-time propagation.

Further evidence for the homogeneity of the total density distribution is also shown in Fig. 4, where we plot the density of the two species $n_A(\theta)$, $n_B(\theta)$, and also the total density distribution $n_A + n_B$, for the values used in Fig. 3 ($x_A = 0.8$, $x_B = 0.2$, and $\gamma = 1250/\pi^2$) and also choosing ℓ to be 0.3. While the density of the two components shows a substantial variation over the ring, the total density is very close to homogeneous, with fluctuations which are of order $1/\gamma$, as we have checked from our data.

VI. DISCUSSION AND CONCLUSIONS

In the present study we have examined the problem of stability of persistent currents of a mixture of two Bose-Einstein condensates which are confined in a ring potential considering the combination $(\Psi_A, \Psi_B) = (\Phi_m, \Phi_n)$.

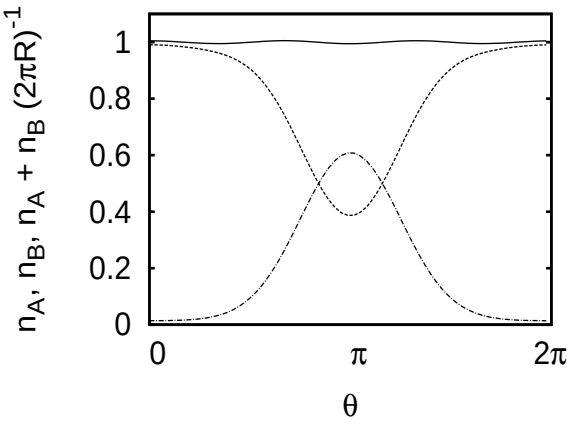

FIG. 4: The density $n_A(\theta)$ (dotted curve), $n_B(\theta)$ (dashed dotted curve), and the total density $n_A(\theta)+n_B(\theta)$ (solid curve), for $\ell = 0.3$, $x_A = 0.8$, $x_B = 0.2$, and $\gamma = 1250/\pi^2$ that results from the method of imaginary time propagation described in Sec. V.

We have thus found that only the case $(\Psi_A, \Psi_B) = (\Phi_m, \Phi_0)$ may give rise to stability of the currents, in agreement with the results of Ref. [12]. The (essentially variational) method that we have used gives insight into this problem, since it avoids solving the two coupled nonlinear differential equations. On the other hand, there is an additional complication, which has to do with the states $(\Psi_A, \Psi_B) = (\Phi_m, \Phi_0)$ being the actual yrast states.

As we have seen, for sufficiently strong interactions and a large population imbalance this combination becomes the yrast state, as seen in the lower curve of Fig. 2, for $m = 2$. For even larger values of the coupling the combination $(\Psi_A, \Psi_B) = (\Phi_m, \Phi_0)$ becomes a local minimum of the dispersion relation, provided that the above solution does not belong to the linear part of the dispersion [9].

In order for our analysis of the stability of the persistent currents to be valid – which investigates the behavior of the system at $\ell \to (mx_A)^-$ – requires that the combination $(\Psi_A, \Psi_B) = (\Phi_m, \Phi_0)$ is the yrast state for $\ell = mx_A$. In the $(x_A - \gamma)$ phase diagram, there are thus two phase boundaries which need to be derived. It turns out that for $n = 0$ the condition for stability of the currents guarantees that the pair $(\Psi_A, \Psi_B) = (\Phi_m, \Phi_0)$ is the yrast state [for $\ell = mx_A$ and $x_A > x_{A,\mathrm{cr}} = 1 - 1/(4m^2)$]. As seen from Fig. 2, for some fixed population imbalance and some fixed angular momentum $\ell = mx_A$, as the coupling increases, first the combination $(\Psi_A, \Psi_B) = (\Phi_m, \Phi_0)$ becomes the yrast state and then it provides a local minimum in the dispersion relation.

Another remarkable and general result of our study is the homogeneity of the total density distribution (see Fig. 4), which characterizes the *whole* yrast spectrum for large values of the coupling constant. In this limit the yrast state has this surprisingly simple feature, in a sense resembling the Tonks-Girardeau limit of fermionized bosons.

Last but not least, it is worth comparing the above results (which assume that $\gamma_{AA} = \gamma_{AB} = \gamma_{BB}$) with the case where these are unequal, which will be examined in a future publication. The main difference (in terms of the applicability) of the main result of this study, i.e., Eq. (9), is when x_B is not sufficiently small. For equal values of the γ_{ij} considered here, stability of persistent currents is not possible. On the other hand, for unequal values of the γ_{ij} metastability may be possible for sufficiently strong interatomic interactions. In addition, the case $n > 0$ may also give rise to persistent currents, as opposed to the present problem. Finally, more local minima may appear in the dispersion relation.

Given that an experiment on this problem has already been performed [8], it would be interesting to investigate whether the interesting structure revealed in the theoretical studies of this problem is indeed observable.

Acknowledgments

We thank Zhigang Wu and Eugene Zaremba for pointing out that the case $n > 0$ requires special care. This project is implemented through the Operational Program "Education and Lifelong Learning", Action Archimedes III and is co-financed by the European Union (European Social Fund) and Greek national funds (National Strategic Reference Framework 2007 - 2013).

[1] S. Gupta, K. W. Murch, K. L. Moore, T. P. Purdy, and D. M. Stamper-Kurn, Phys. Rev. Lett. **95**, 143201 (2005).
[2] Spencer E. Olson, Matthew L. Terraciano, Mark Bashkansky, and Fredrik K. Fatemi, Phys. Rev. A **76**, 061404(R) (2007).
[3] C. Ryu, M. F. Andersen, P. Cladé, Vasant Natarajan, K. Helmerson, and W. D. Phillips, Phys. Rev. Lett. **99**, 260401 (2007).
[4] B. E. Sherlock, M. Gildemeister, E. Owen, E. Nugent, and C. J. Foot, Phys. Rev. A **83**, 043408 (2011).
[5] A. Ramanathan, K. C. Wright, S. R. Muniz, M. Zelan, W. T. Hill, C. J. Lobb, K. Helmerson, W. D. Phillips, and G. K. Campbell, Phys. Rev. Lett. **106**, 130401 (2011).
[6] Stuart Moulder, Scott Beattie, Robert P. Smith, Naaman Tammuz, and Zoran Hadzibabic, Phys. Rev. A **86**, 013629 (2012).
[7] C. Ryu, K. C. Henderson and M. G. Boshier, New J. Phys. **16**, 013046 (2014).
[8] Scott Beattie, Stuart Moulder, Richard J. Fletcher, and Zoran Hadzibabic, Phys. Rev. Lett. **110**, 025301 (2013).
[9] J. Smyrnakis, S. Bargi, G. M. Kavoulakis, M. Magiropoulos, K. Kärkkäinen, and S. M. Reimann, Phys. Rev. Lett.

103, 100404 (2009).
[10] F. Bloch, Phys. Rev. A **7**, 2187 (1973).
[11] K. Anoshkin, Z. Wu, and E. Zaremba, Phys. Rev. A **88**, 013609 (2013).
[12] Zhigang Wu and Eugene Zaremba, Phys. Rev. A **88**, 063640 (2013).
[13] A. D. Jackson, J. Smyrnakis, M. Magiropoulos, and G. M. Kavoulakis, Europh. Lett. **95**, 30002 (2011).
[14] We stress here that when we refer to "large" values of the coupling we restrict ourselves to the case where, although γ is large, still $\gamma \ll N^2$, so that the gas is still in the mean-field limit, away from the Tonks-Girardeau regime.
[15] S. Komineas, N. R. Cooper, and N. Papanicolaou, Phys. Rev. A **72**, 053624 (2005).